Label-Efficient Grasp Joint Prediction with Point–JEPA

Jed Guzelkabaagac
Technical University of Munich
Munich, Germany
jed.guzelkabaagac@tum.de

Boris Petrović
Technical University of Munich
Munich, Germany
boris.petrovic@tum.de

***Abstract*—We study whether 3D self-supervised pretraining with a Joint-Embedding Predictive Architecture (Point–JEPA) enables label-efficient grasp joint-angle prediction. Meshes are converted to point clouds and tokenized; a ShapeNet-pretrained Point–JEPA encoder feeds a lightweight $K{=}5$ multi-hypothesis head trained with winner-takes-all and evaluated by top–logit selection. On DLR–Hand II with strict object-level splits, Point–JEPA improves top–logit RMSE and Coverage@15° in low-label regimes (e.g., 26% lower RMSE at 25% data) and reaches parity at full supervision. This suggests JEPA-style pretraining is a practical lever for data-efficient grasp learning.**

I. Related Work

Self-supervised learning (SSL) for 3D data has largely progressed along three directions.

(i) Reconstruction-based methods learn by masking and reconstructing inputs in the input space. On point clouds this includes point/voxel masked autoencoding; e.g., Voxel-MAE reconstructs masked voxels for sparse automotive LiDAR and improves downstream tasks with fewer labels [1]–[4].

(ii) Teacher–student (latent-target) objectives predict contextualized *latent* targets rather than raw inputs. data2vec provides a modality-agnostic recipe that predicts latent representations of the full input from a masked view, while Point2Vec adapts this idea to point clouds and addresses positional-leakage pitfalls unique to 3D, reporting strong transfer on ModelNet40/ScanObjectNN [5], [6].

(iii) Joint-embedding predictive architectures (JEPA) predict target *representations* for spatially contiguous blocks from a single context block, learning semantic features without heavy view augmentations [7], [8]. Point–JEPA brings this design to point clouds with a simple sequencer that orders patch centers so contiguous context/target blocks can be sampled despite unordered points, avoiding input-space reconstruction or extra modalities while remaining competitive on standard 3D benchmarks [8], [9].

Despite this progress, the impact of predictive, context-aware pretraining on *grasp–joint prediction* remains under-explored [10]–[12]. In this study, we adopt a Point–JEPA backbone for object embeddings and pair it with an inference-aware, multi-hypothesis loss for joint angles, comparing against training from scratch and analyzing label-efficiency gains under fixed object-level splits.

[1] code & figures (https://github.com/jedguz/Point-JEPA-grasping).

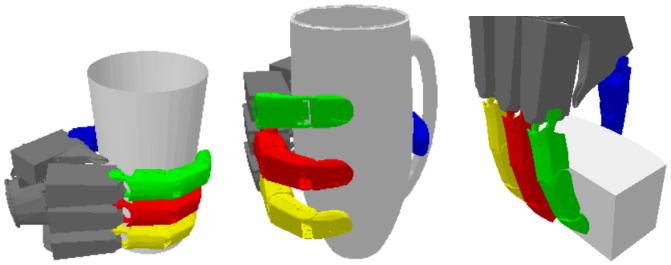

(a) (b) (c)

Fig. 1: **Qualitative predictions.** Conditioned on an object mesh and a given *7D* hand/wrist pose (3D position + unit quaternion), the model predicts a *12D* joint-angle vector that yields a stable, collision-free grasp. Panels (a–c) show the *top-logit* hypothesis ($K{=}5$) for three object–pose pairs.

II. Technical Outline

We convert meshes to point clouds and tokenize them into local patches for transformer processing [13].

We utilize a pretrained JEPA backbone trained on ShapeNet point clouds via Point–JEPA [9]. A block sampler selects *spatially contiguous* target windows, and a sequencer orders patch centers to keep these windows contiguous in the token sequence, following the JEPA masking/targeting scheme [7]. The *context encoder* sees masked input; the *target encoder* sees full input to produce latent targets. A lightweight predictor maps context features to the target space; we regress predictions to stop-gradient targets on masked blocks. The target encoder is an EMA copy of the context encoder; no negatives or input reconstruction are required. After pretraining we discard the predictor and EMA target, retaining the context encoder for contextualized patch features (Fig. 2); attention pooling yields a global object embedding (Fig. 3). For clarity, Fig. 2 depicts single masked patches; training uses block masking.

For grasp prediction, the pooled object embedding is concatenated with the 7D wrist pose and passed to a lightweight head that emits K joint-angle hypotheses and logits. Training uses a winner-takes-all / min-over-K objective to preserve multi-modality (see Sec. III-D); at inference, we select the top–logit hypothesis [14].

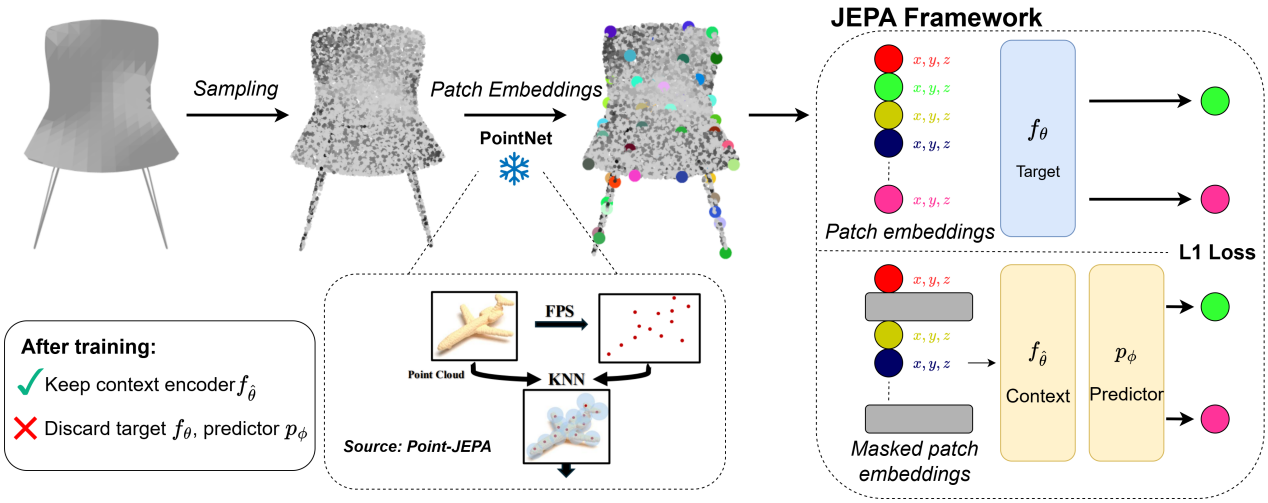

Fig. 2: **Point–JEPA pretraining [9].** Object mesh is converted to a point cloud, tokenized into patch embeddings, and passed to a self-distilled JEPA to obtain contextualized patch features.

III. Methodology

A. Dataset & split protocol

Data and filtering. We use the DLR–Hand II dataset *(non-public; for code/protocol/weights see Footnote 1)* built atop ShapeNet object categories, comprising a range from 10 to 500 unique shapes per category. Each shape provides around 240 grasp samples, each consisting of a 7D wrist pose, a 12D joint configuration, and a grasp quality score. After discarding all grasps with score < 1.5, our dataset contains on the order of 1,500 meshes and 370,000 total grasps.

Object-level, category-stratified splits. To prevent overfitting and pose leakage from multiple grasps of the same mesh, we split at the object level. Sample-level splits proved overly easy and invalidated the value of SSL-based encoding, and so were not used.

Fixed evaluation. We fix one suite consistent for all label budgets: *val* (10% of objects) and *test* (another 10%).

Low–data training subsets. For $p \in \{1, 10, 25, 100\}\%$, we sample the train set from the remaining objects with proportional *category stratification* (at least one object per synset).

Two split packs and reproducibility. We construct two independent train split packs (A/B) with different manifest seeds; validation fixtures (val, test) are identical across packs. Unless otherwise stated, entries report the mean $\pm$ SD over initialization seeds (0,1) and, where available, over split packs. Due to compute constraints, Pack B was run at *anchor budgets* (25% and 100%); the low-label budgets (1%, 10%) use Pack A. At the anchor points, Pack A and Pack B yield qualitatively similar trends, so we adopt Pack A as the default and use Pack B to check pack sensitivity.

B. Preprocessing & object representation

Meshes are converted to point clouds and tokenized into local groups to create patch embeddings. We use 1024 points per object and a tokenizer with 64 groups (group size 32, radius 0.05). These patch embeddings feed the self–supervised encoder (Fig. 2); a global object embedding is then produced by *attention pooling*, which we found to be more stable and accurate than mean/max pooling.

C. SSL backbone (Point–JEPA)

We use the Point–JEPA *context encoder* as the backbone (predictor/target discarded after pretraining). Tokenized point-cloud patches with positional encodings are encoded and attention-pooled into a single object embedding. We fine-tune end-to-end with a *two-tier learning rate* (smaller on the pretrained backbone, larger on the new grasp head); concrete settings and schedules appear in Sec. IV.

D. Joint estimation head & loss

We predict K candidate joint configurations $\{\hat{\mathbf{j}}_k\}_{k=1}^{K}$ for each object embedding and wrist pose, together with a logit vector $\boldsymbol{\ell} \in \mathbb{R}^K$ used to rank hypotheses at test time. Grasping is inherently *multi-modal*: several distinct joint settings can succeed for the same pose, and single-output MSE collapses these modes to their mean, often yielding an interpolated (and infeasible) grasp (see Fig. 4). To preserve distinct modes, we use a winner-takes-all (WTA) / min-over-K objective, a standard approach for ambiguous prediction tasks.

$$k^* = \arg\min_k \|\hat{\mathbf{j}}_k - \mathbf{j}\|^2 \tag{1}$$

$$L = \|\hat{\mathbf{j}}_{k^*} - \mathbf{j}\|^2 + \alpha\, \mathrm{CE}(\boldsymbol{\ell},\, k^*) \tag{2}$$

The first term penalizes only the closest hypothesis, avoiding mean-collapse; the cross-entropy term teaches the logits to act as a proxy selector for the winning mode. We then use the *same* selector at inference (pick the top–logit hypothesis), so evaluation does not rely on an oracle "best-of-K". This mirrors multi-hypothesis practice in trajectory forecasting, where sets of candidates are scored and one is chosen at test time.

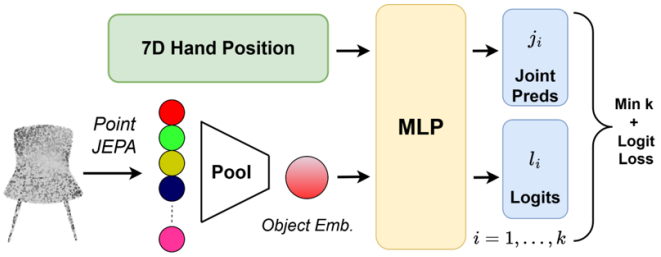

Fig. 3: **Grasp head architecture.** Contextualized object features from Point–JEPA are pooled into a global embedding and concatenated with the 7D wrist pose. An MLP predicts K joint configurations and corresponding logits.

In preliminary trials we also considered Mixture Density Networks (MDNs) to model multi-modality probabilistically, but found them brittle in this high-dimensional joint space (training instability and covariance issues) and less aligned with our top-1 selection at inference; the WTA formulation remained simpler and more stable.

All experiments use $K{=}5$ to balance coverage and compute (brief pilots with $K \in \{3, 4\}$ were inconclusive; a full sweep is left to future work). Beyond the primary top–logit RMSE, we report two diagnostics that probe the multi-hypothesis mechanism without relying on an oracle at evaluation time: (i) a *selection gap* (top–logit RMSE minus best-of-K RMSE) to assess selector fidelity, and (ii) *Coverage*@15°, the fraction of samples for which at least one hypothesis lies within 15° of the ground truth.

E. Evaluation protocol & metrics

At inference, we choose the head with the largest logit ("top–logit"). The main metric is **top–logit RMSE** on joint angles. We additionally compute *coverage*@$\{10°, 15°, 20°\}$ (a grasp counts as covered if any head is within the angular threshold) and a diversity proxy (mean pairwise dispersion across heads) to quantify multimodality.

IV. Results

All metrics are reported on the fixed *test* split with object-level stratification, averaged over split packs and seeds where available.

A. Main outcomes

Table I summarizes top–logit RMSE (radians; lower is better). Three patterns emerge:

- **Low labels (1–10%):** JEPA pretraining yields consistent gains (≈8–10% relative error reduction), indicating improved label efficiency in scarce-data regimes.
- **Moderate labels (25%):** The largest improvement appears at 25% (≈26% relative), a "sweet spot" where pretrained context helps most before fully supervised training saturates.
- **Full labels (100%):** Performance is effectively at parity; differences are within seed variance (JEPA ≈ scratch), suggesting that with enough supervision, training from random initialization can catch up.

TABLE I: **Top–logit RMSE (rad) across label budgets.** Means ± SD over seeds; budgets marked † average across Packs A+B (25%, 100%), while 1% and 10% use Pack A only.

Train split	Scratch	JEPA	Δ (rel.)
1%	0.363 ± 0.002	**0.335 ± 0.003**	+7.7%
10%	0.335 ± 0.003	**0.303 ± 0.009**	+9.6%
25%†	0.332 ± 0.002	**0.246 ± 0.012**	+25.9%
100%†	0.235 ± 0.002	**0.234 ± 0.008**	+0.4%

B. Inference-aware selection and coverage

To assess whether the logits reliably choose the correct hypothesis, we define the *selection gap*

$$\Delta_{\text{sel}} = \text{RMSE}_{\text{top–logit}} - \text{RMSE}_{\text{best-of-}K},$$

with smaller values indicating better alignment between the learned selector and the oracle winner. At 1% and 10% budgets, JEPA reduces the gap relative to scratch (e.g., 1%: 0.142 vs 0.165 rad; 10%: 0.157 vs 0.176 rad), demonstrating stronger inference-aware selection. The full curves and plotting scripts are provided in our Git repository.

As a complementary multi-hypothesis metric, we report Coverage@15°: a grasp is covered if *any* head lies within 15° of the ground-truth joint angles. Coverage increases with label budget and is consistently higher with JEPA in the low-label settings (e.g., at 10%: 0.955 vs 0.938; at 1%: 0.866 vs 0.861); see the repository for the corresponding curves and scripts.

C. Sensitivity to learning rates (10% grid)

We ran a 3×2 grid over $(\text{LR}_{\text{backbone}}, \text{LR}_{\text{head}})$ on the 10% split (time constraints precluded repeating per budget). Top–logit RMSE versus training step shows a broad plateau at convergence: final differences across the grid are small ($\lesssim$ 0.01 rad). Larger backbone LRs destabilize early fine-tuning, while smaller head LRs slow convergence. We therefore fix $(\text{LR}_{\text{backbone}}, \text{LR}_{\text{head}}) = (1{\times}10^{-5}, 1{\times}10^{-3})$ for all budgets.

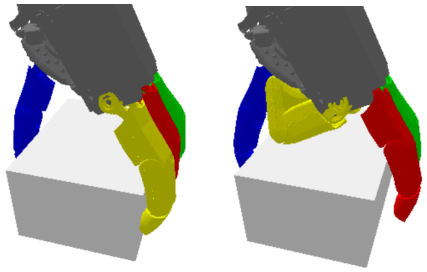

(a) (b)

Fig. 4: **Min-over-K illustrated.** For a fixed object and wrist pose, two hypotheses $(\hat{\mathbf{j}}_1, \hat{\mathbf{j}}_2)$ yield stable, collision-free grasps (a–b), while their mean is infeasible. Training (Eq. 2) regresses only the hypothesis nearest to $\mathbf{j}$ by L2 in joint-angle space and trains logits via cross-entropy; inference uses the top–logit.

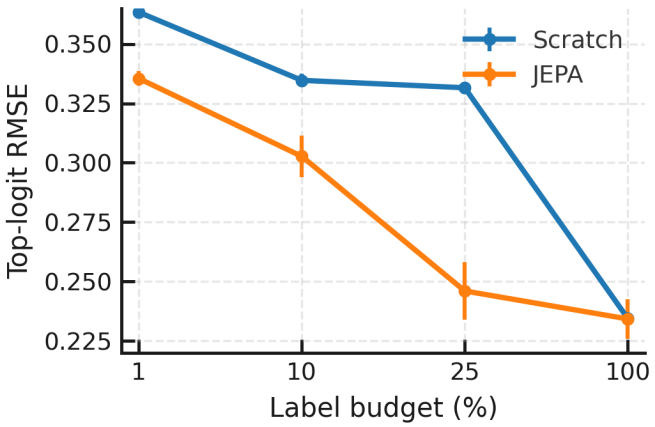

Fig. 5: **Label efficiency.** Test top–logit RMSE versus label budget (1%, 10%, 25%, 100%). JEPA pretraining improves performance in low-label regimes, with the largest gap at 25%; at 100% both methods converge. Points show mean over seeds/split packs; error bars denote ± 1 SD.

V. Conclusion

We investigated whether 3D self-supervised pretraining improves grasp-joint prediction under limited labels. Integrating a Point–JEPA backbone with a winner-takes-all multi-hypothesis head yields consistent gains in low-label regimes on DLR–Hand II, with the largest relative improvement at 25% data. At 100% labels, training from scratch attains parity. Diagnostics indicate that the selector is effective (smaller selection gap) and that Coverage@15° improves with pretraining, supporting the inference-aware design.

Results indicate JEPA-style pretraining is a practical label-efficiency lever for grasping systems when annotation is expensive.

VI. Future work

We outline several directions to strengthen generalization and deployment relevance:

- **Cross-domain evaluation.** Run the pre-registered *test_category* suite and real-robot tests to assess transfer beyond object-level splits.
- **Heads and selection.** Sweep K and study diversity-encouraging variants, while monitoring selection gap and top–logit coverage as primary inference-aware metrics.
- **Geometry-aware patching.** Replace FPS + fixed-kNN with patches built from simple geometric cues, e.g., multi-scale radius neighborhoods, curvature-guided grouping, and small overlaps, so each patch better respects local shape.
- **Geometry-focused tokenizer.** Swap the PointNet patch encoder for one that uses explicit local geometry. The JEPA objective stays the same; only the patch encoder changes.
- **Compute-efficient fine-tuning.** Evaluate lightweight adaptation (e.g., LoRA) and backbone LR schedules across label budgets.

References

[1] G. Hess, J. Jaxing, E. Svensson, D. Hagerman, C. Petersson, and L. Svensson, "Masked autoencoder for self-supervised pre-training on lidar point clouds," in *2023 IEEE/CVF Winter Conference on Applications of Computer Vision Workshops (WACVW)*. IEEE, 2023, pp. 350–359.

[2] Z. Xie *et al.*, "Masked autoencoders for point cloud self-supervised learning," in *Proceedings of the IEEE/CVF Conference on Computer Vision and Pattern Recognition (CVPR)*, 2022.

[3] X. Yu *et al.*, "Point-bert: Pre-training 3d point cloud transformers with masked point modeling," in *Proceedings of the IEEE/CVF Conference on Computer Vision and Pattern Recognition (CVPR)*, 2022.

[4] Y. Liu *et al.*, "Maskpoint: Masked autoencoders for point cloud self-supervised learning," in *Proceedings of the IEEE/CVF International Conference on Computer Vision (ICCV)*, 2023.

[5] A. Baevski, W.-N. Hsu, Q. Xu, A. Babu, J. Gu, and M. Auli, "data2vec: A general framework for self-supervised learning in speech, vision and language," *arXiv preprint arXiv:2202.03555*, 2022.

[6] K. Abou Zeid, J. Schult, A. Hermans, and B. Leibe, "Point2vec for self-supervised representation learning on point clouds," 2023.

[7] M. Assran, Q. Duval, I. Misra, P. Bojanowski, P. Vincent, M. Rabbat, Y. LeCun, and N. Ballas, "Self-supervised learning from images with a joint-embedding predictive architecture," 2023.

[8] N. Hu, H. Cheng, Y. Xie, S. Li, and J. Zhu, "3d-jepa: A joint embedding predictive architecture for 3d self-supervised representation learning," 2024.

[9] A. Saito, P. Kudeshia, and J. Poovvancheri, "Point-jepa: A joint embedding predictive architecture for self-supervised learning on point cloud," 2025.

[10] J. Mahler *et al.*, "Dex-net 2.0: Deep learning to plan robust grasps with synthetic point clouds and analytic grasp metrics," in *Robotics: Science and Systems (RSS)*, 2017.

[11] M. Gualtieri, A. Ten Pas, K. Saenko, and R. Platt, "High precision grasp pose detection in dense clutter," in *IEEE International Conference on Robotics and Automation (ICRA)*, 2016.

[12] M. Sundermeyer, A. Mousavian, and D. Fox, "Contact-graspnet: Efficient 6-dof grasp generation in cluttered scenes," in *IEEE International Conference on Robotics and Automation (ICRA)*, 2021.

[13] C. R. Qi, L. Yi, H. Su, and L. J. Guibas, "Pointnet++: Deep hierarchical feature learning on point sets in a metric space," in *Advances in Neural Information Processing Systems (NeurIPS)*, 2017.

[14] T. Phan-Minh *et al.*, "Covernet: Multimodal behavior prediction using trajectory sets," in *IEEE International Conference on Robotics and Automation (ICRA)*, 2020.